THE JOURNAL OF PHYSICAL CHEMISTRY Letters

Letter

pubs.acs.org/JPCL

Surface-Heating Algorithm for Water at Nanoscale

Sumith YD and Shalabh C. Maroo*

Department of Mechanical and Aerospace Engineering, Syracuse University, Syracuse, New York 13244, United States

Supporting Information

ABSTRACT: A novel surface-heating algorithm for water is developed for molecular dynamics simulations. The validated algorithm can simulate the transient behavior of the evaporation of water when heated from a surface, which has been lacking in the literature. In this work, the algorithm is used to study the evaporation of water droplets on a platinum surface at different temperatures. The resulting contact angles of the droplets are compared to existing theoretical, numerical, and experimental studies. The evaporation profile along the droplet's radius and height is deduced along with the temperature gradient within the drop, and the evaporation behavior conforms to the Kelvin−Clapeyron theory. The algorithm captures the realistic differential thermal gradient in water heated at the surface and is promising for studying various heating/cooling problems, such as thin film evaporation, Leidenfrost effect, and so forth. The simplicity of the algorithm allows it to be easily extended to other surfaces and integrated into various molecular simulation software and user codes.

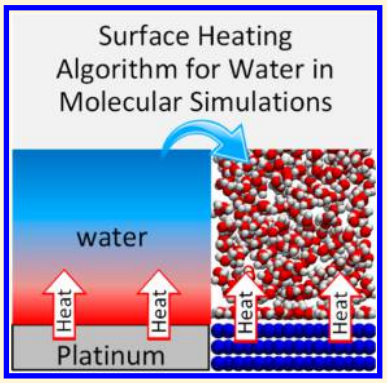

Molecular dynamics (MD) simulations are a powerful computational tool for solving numerous problems in science and engineering, especially at nanoscale. In MD simulations that involve liquids, the canonical ensemble is most commonly simulated by coupling the liquid to an external thermostat.[1,2] However, thermostats cannot be used to study nonequilibrium phenomena, and thermostatting of liquid interacting with frozen solid surfaces may give unrealistic results.[3,4] Nonequilibrium MD simulations on the surface evaporation of liquids have been largely focused on using simple nonpolar Lennard-Jones fluids.[5−8] Water, although a more practical fluid of interest, has only been the focus of a handful of surface evaporation studies[9−11] primarily due to the presence of electrostatic forces and its complex nature of interaction. Among them, the phantom wall method,[7] which uses Langevin-based scaling for phantom layers of platinum, has been used to simulate the heat transfer between a surface and water.[12] Luca et al.[10] developed a virtual particle-based algorithm that heats confined water in between parallel plates where virtual particles interact with water by oscillating normal to the wall, transferring the kinetic energy; the water domain height studied was <2 nm thick. Wang et al.[13] simulated the evaporation of water droplets using an accelerated region where the molecules falling between a region above the surface accelerated with a prespecified force away from the surface. However, these surface heating models of water do not capture the heat transfer characteristics and thermodynamic properties of water evaporation. Moreover, these methods, which simulate the wall atomic vibrations, are (1) questionable as the integration time steps of both solid and liquid are assumed to be the same even though their atomic vibrational frequencies differ significantly,[14,15] and (2) computationally very expensive due to the high frequency vibrations. Thus, correctly simulating the transient behavior of water evaporation requires the application of a combination of frozen wall and appropriate thermal wall algorithms. In this work, we propose a novel algorithm to simulate heat transfer from a heated platinum surface (in the temperature range of 300−400 K) to water droplets and validate the algorithm by contact angle estimation, comparison with the classical one-dimensional heat equation, and analysis of the evaporation profile and temperature gradient in the droplet.

The simulated domain comprises a water droplet on a platinum surface (Figure 1a). Water is modeled using rigid SPCE[16] molecules. The platinum surface is modeled as 3-layers of FCC 111 lattice and forms the lower boundary. The top boundary is adiabatic (reflective), and all sides are periodic in nature (the reflective boundary is applied by reversing the atom's direction of velocity normal to the surface). Two molecular systems are considered: (1) a 64 nm^3 droplet, initially as a cube of water on top of a platinum surface of dimension 20 × 20 nm, and (2) a 216 nm^3 droplet, of side 6 nm on a 25 × 25 nm platinum surface. The droplet is equilibrated for 1000 ps on the platinum surface (Figure 1a). Water−water interaction is modeled using the modified shifted Coulomb potential[17] with a cutoff radius of 1.1 nm. The numerical integration is performed using the velocity Verlet scheme. The rigid molecules are simulated using the RATTLE-constrained algorithm.[18] The interaction between platinum and water is modeled using Zhu Philpott (ZP) potential[19] (please refer to Supporting Information) as it gives accurate interaction energy between water and platinum atoms. An in-house C++ code was developed for all the simulations performed in this work.

The development of a heat transfer model for ZP potential is not straightforward due to the potential's anisotropic nature.

Received: July 29, 2015
Accepted: September 3, 2015
Published: September 3, 2015

DOI: 10.1021/acs.jpclett.5b01627
J. Phys. Chem. Lett. 2015, 6, 3765−3769

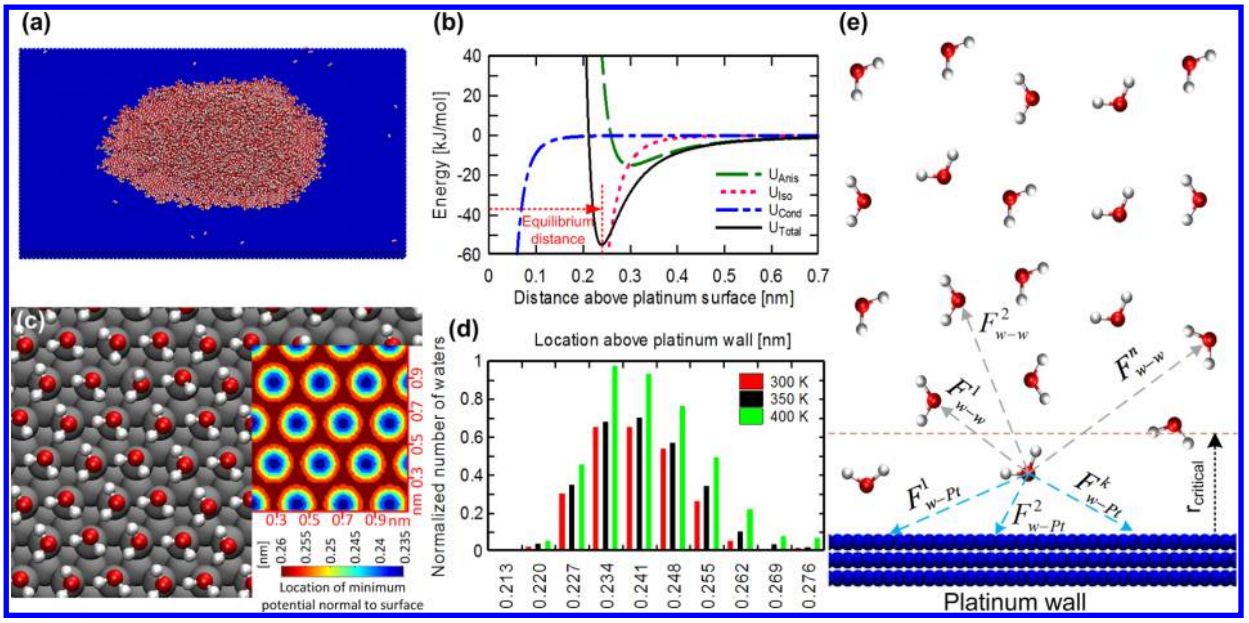

Figure 1. Water−surface interaction and the new surface heating algorithm for water. (a) An equilibrated droplet of 7221 water molecules on top of the platinum surface (in blue). This droplet was initially a 6 nm side cube and then equilibrated for 1000 ps at a surface temperature of 300 K. (b) ZP potential energy and its components based on the interaction of a flat-oriented SPCE[16] water molecule with the platinum surface. (c) Orientation of water molecules in the monolayer above the platinum surface showing that the majority of the water molecules are in a flat-orientation along with the minimum potential contours of flat-oriented water molecules. The blue regions in the contour have the strongest attraction and act as the adsorption sites for water to form the monolayer. (d) Frequency distribution of water molecules in the monolayer above the platinum surface at different surface temperatures; the number density is normalized by a factor of 1000. (e) Graphical representation of the surface heating algorithm for water; F^{n}_{w-w} represents the interaction force between a water molecule in the critical radius region and the n^{th} water molecule, and F^{k}_{w-Pt} represents the interaction between the same water molecule and k^{th} platinum atom.

Figure 1b shows the ZP potential energy function and its components for a flat water molecule (hydrogens and oxygen of the molecule lying on a plane parallel to platinum surface). The ZP potential influences the structure of water adsorbed on the platinum surface and is of significant importance for developing a surface heating algorithm. Figure 1c shows the orientation of the dense single layer of adsorbed water molecules, generally known as a monolayer, with minimum potential contour for a flat water orientation. The structure of the monolayer has a majority of the water molecules in the flat orientation. The monolayer position varies by less than an angstrom based on the water molecular distribution histograms (Figure 1d) for different surface temperatures studied in this work.

The central idea of the new algorithm is shown graphically in Figure 1e. A "critical zone" is defined as the region above the platinum wall up to a distance of $r_{critical}$. For the water molecules lying in the critical zone, the net force acting on the molecule from the surface is compared with the force acting on it from all other water molecules. If the force due to the surface is larger, the water molecule will be heated (or cooled) to the platinum surface temperature using the velocity scaling method. Thus, a water molecule is heated (or cooled) by the surface if the following two criteria are met

$$z_{oxygen} < r_{critical} \tag{1}$$

$$\sum_{i=1}^{k} F^{i}_{w-Pt} > \sum_{j=1}^{n} F^{j}_{w-w} \tag{2}$$

where k is the number of platinum atoms, n is the number of water molecules, F_{w-Pt} and F_{w-w} represent the force interaction between individual molecules for water−platinum and water−water, respectively. The basis of this new algorithm is derived from a validated surface-heating algorithm by Maroo and Chung,[20] which was used, however, for simpler nonpolar LJ argon fluid heat transfer. Unlike argon, a unified critical radius region (minimum potential), $r_{critical}$, is not analytically possible for water−platinum interactions as the ZP potential is anisotropic. Thus, we performed multiple MD simulations to empirically estimate $r_{critical}$ for the surface heating algorithm for water.

For the estimation of the critical radius, a 4 nm cube of water was equilibrated on the platinum surface until it formed a water droplet. The new surface-heating algorithm was applied for a surface temperature of 300 K, and $r_{critical}$ was varied from 0.248 to 0.257 nm. This range of $r_{critical}$ was selected from the positional distribution of water molecules in the monolayer (Figure 1d) and the minimum potential energy location of an individual water molecule. The equilibrated droplet temperature was measured by varying $r_{critical}$, and the same procedure was repeated for surface temperatures of 350 and 400 K (Figure 2a). Using linear fits, the appropriate $r_{critical}$ was chosen when the surface temperature and droplet temperature matched. Thus, an $r_{critical}$ value for each temperature was obtained from which a correlation was deduced based on a linear fit (Figure 2b). Hence, the following correlation can be used to determine $r_{critical}$ for a desired surface heating temperature

$$r_{critical} = 0.000072 \times T + 0.225133 \tag{3}$$

where T is the temperature of the platinum surface (300 K $\leq T \leq$ 400 K). The implementation of this algorithm is included in the Supporting Information as a pseudo code.

The next step was to validate and demonstrate that this new algorithm produces physically sound results. On the basis of the above correlation, additional simulations were performed for

DOI: 10.1021/acs.jpclett.5b01627
J. Phys. Chem. Lett. 2015, 6, 3765−3769

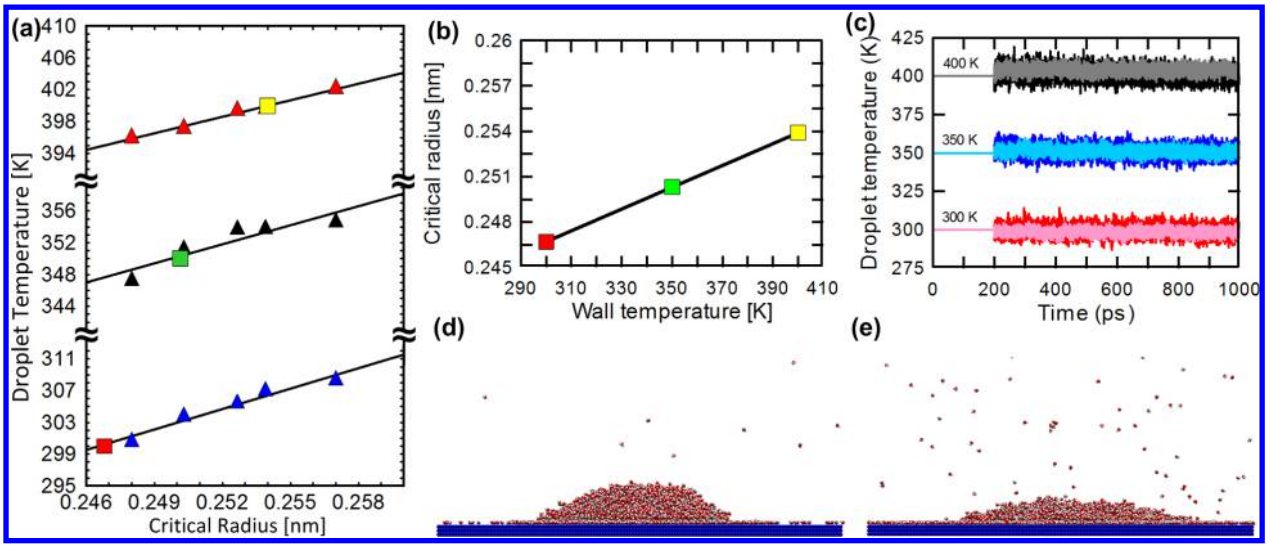

Figure 2. Estimation of the critical radius for the surface heating algorithm of water. (a) Droplet temperatures with varying critical radius while maintaining the surface temperature at 300 K (blue triangles), 350 K (black triangles), and 400 K (red triangles). The linear fits for these data are shown as solid lines. Interpolated critical radius values are shown in solid squares when the droplet temperature matches the surface temperature. (b) Correlation between critical radius and surface temperature based on data from (a), which can be used to determine the required critical radius for a desired surface temperature. (c) Temperature evolution of droplets with velocity scaling for the first 200 ps and the surface heating algorithm thereafter. The darker colored lines represent the data for the 64 nm^3 volume droplet, and the lighter colored lines represent the 216 nm^3 droplet at the 300, 350, and 400 K surface temperatures. Evaporation of the 216 nm^3 droplet at (d) 350 K and (e) 400 K surface temperature (images taken at 1000 ps).

surface temperatures of 300, 350, and 400 K with 4 and 6 nm cube droplets. Temperature evolution of the water droplets is shown in Figure 2c. The equilibrated water droplet's mean temperature (Table 1) shows the accuracy of the proposed algorithm; the maximum error (deviation of average from the expected surface temperature) is less than 1%. Evaporation of the droplets was also observed for surface temperatures of 350 and 400 K in Figure 2d and e, respectively. To the best of our knowledge, there is no prior work reported for evaporation of water droplets based on surface heating in MD simulations. The algorithm was also validated using the classical one-dimensional heat equation (please refer to the Supporting Information).

Table 1. Water Droplet Temperature at Steady State Using the Surface Heating Algorithm for the Two MD Systems Studied (64 nm^3 and 216 nm^3 Droplet Volumes)

	droplet temperature (K)		
surface temperature (K)	64 nm^3	216 nm^3	|max. error|
300	299.4 ± 3.2	298.5 ± 1.8	0.5%
350	350.7 ± 3.3	350.9 ± 2.1	0.3%
400	400.8 ± 3.5	403.9 ± 2.2	1.0%

The algorithm was further validated by studying the dependency of the contact angle of the water droplets at different platinum surface temperatures (300, 350, and 400 K). Contact angle studies are important for understanding wettability and surface interaction energies. There are many studies on the contact angle of water on graphene,[21,22] graphite,[23] carbon nanotubes,[24,25] solid surfaces,[26,27] polymer surfaces,[28] and platinum[9,29] using molecular dynamics simulations. However, these studies involve equilibrium MD simulations for contact angle determination rather than transient surface-heating nonequilibrium MD as performed in this work. We developed[30] a fast and accurate algorithm to estimate the contact angle, which is applied here. Further, at each time step, the droplet is rotated about the axis normal to the surface with 1° increments up to 90°, and the 2D density-based contact angle is estimated. The curvature is fitted assuming a circular shape with a robust geometric fit algorithm.[31] The contact angle values are temporally averaged from 600 to 1000 ps at every 1 ps. This procedure provides an accurate estimation of the contact angle even for a small droplet undergoing high fluctuations at the liquid vapor interface. Figure 3a shows a screenshot of a water droplet on the platinum surface, equilibrated at a surface temperature of 300 K, with the bold line representing the circle fit based on the

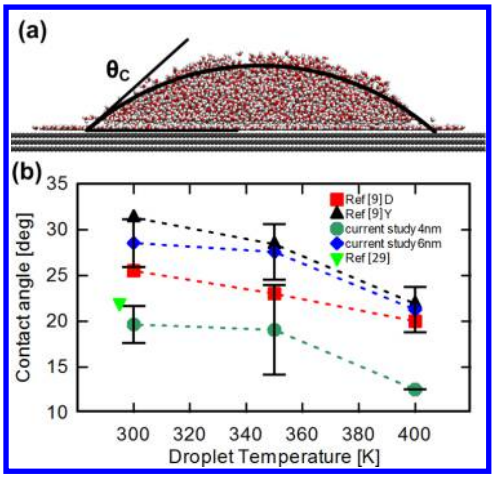

Figure 3. Droplet contact angle estimation and comparison. (a) Water droplet equilibrated at 300 K with the solid curved line depicting the liquid–vapor interface. (b) Contact angle of the droplets at different surface temperatures and comparison with literature. The green and blue curves show the data for 64 and 216 nm^3 droplets, respectively, in the present study. The error bars indicate one standard deviation. D and Y in ref 9 represent data from a direct molecular simulation and from the Young–Laplace equation, respectively. The green triangular marker shows the available experimental data.[29]

DOI: 10.1021/acs.jpclett.5b01627
J. Phys. Chem. Lett. 2015, 6, 3765–3769

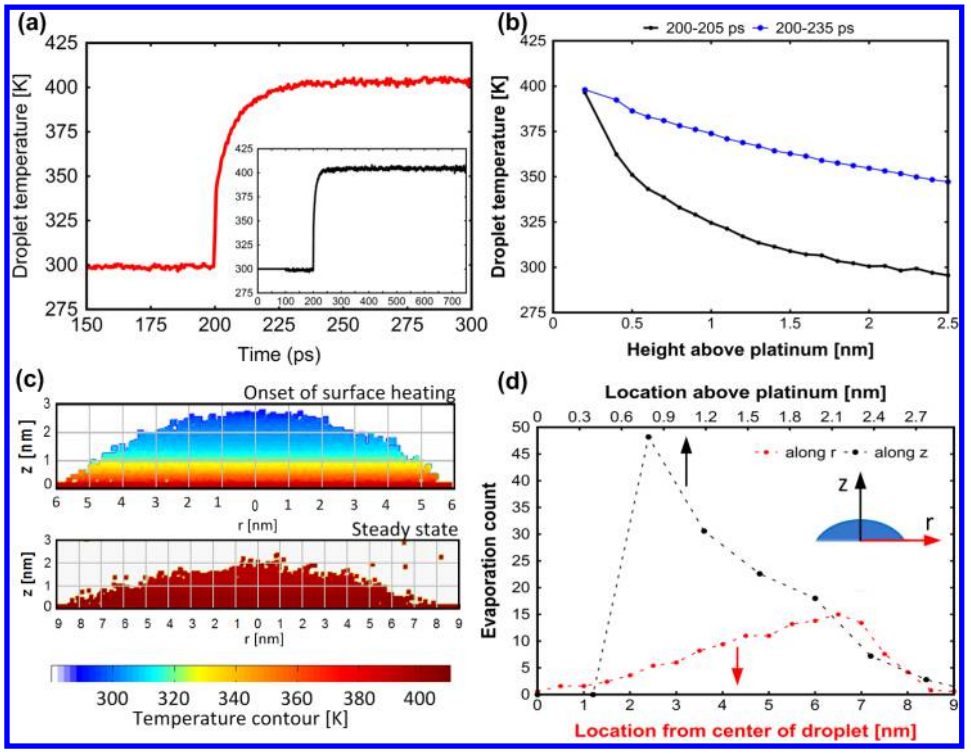

Figure 4. Transient behavior of water droplet evaporation using the surface-heating algorithm. (a) Average droplet temperature variation over time of a 216 nm^3 droplet when the surface is heated from 300 to 400 K. The inset shows the droplet temperature for the entire time range of the simulation. (b) The droplet temperature gradient along the droplet height based on temporal averages from 200 to 205 ps and from 230 to 235 ps. (c) Thermal gradient contours at the onset of surface temperature increase (upper) and for the equilibrated droplet (lower), showing a gradual and realistic change in droplet temperature due to the surface heating when compared to heating the entire droplet using a thermostat. (d) The total number of water molecules evaporated between 200 to 1000 ps (averaged over 5 different simulation sets) plotted against the location of evaporation in the vertical direction (along z) and also from the center of the droplet (along r).

interface identification algorithm. The equilibrated droplet contact angles for different surface temperatures are plotted in Figure 3b. The contact angles are in good agreement with the theoretical model of the Young−Laplace equation,[32,33] prior numerical studies,[9] and experimental measurements.[34]

The algorithm was applied to study the transient behavior of the water droplet evaporation using the 216 nm^3 droplet system. The platinum surface temperature was maintained at 300 K from 0 to 200 ps, following which, the surface temperature was changed to 400 K. This resulted in a gradual increase in the temperature of the droplet, which initiated evaporation. The transient droplet temperature profile is shown in Figure 4a with the droplet reaching a steady state temperature at ∼250 ps. The temperature gradients within the droplet during the transient period of 200−205 ps and 200−235 ps are averaged and plotted in Figure 4b. The distribution shows an exponential-like trend in the temperature of droplets in the initial 5 ps, and a linear change over the larger time period, as expected. Temperature contours of the thermal gradient within the droplet are shown in Figure 4c at the onset of heating and after the droplet reached steady state. As expected at continuum scale, the droplet spreads over the surface at the higher temperature and achieves a uniform temperature in steady state.

The evaporation profile of the droplet was determined with respect to the distance above platinum (labeled as the z-axis) as well as around the centroid of the droplet (labeled as the r-axis). An "evaporated" molecule was defined when a molecule suddenly has one or few neighbors within its 0.4 nm radius near the droplet interface or has less than three neighbors within its 0.4 nm radius away from the droplet. On the basis of this definition, the evaporation positions of all "evaporated" molecules are identified and quantified as shown in Figure 4d. The curve "along z" represents the number of molecules evaporated at positions along the vertical direction, whereas the "along r" curve shows the same data radially outward from the center of the droplet. Both of these curves indicate that the base of the droplet has a higher rate of evaporation primarily due to the higher temperature and thinner water film at the base as seen in Figure 4c. These results are in agreement with the classical Kelvin−Clapeyron equation,[35] where the evaporation rate for a droplet can be approximated as $\dot{m} = a(T_{lv} - T_v) = (1/(1 + (ah_m/k)\delta))a(T_s - T_v)$, where T_{lv} is the liquid−vapor interface temperature, T_v is the vapor temperature, T_s is the surface temperature, δ is the liquid thickness, k is the thermal conductivity of the liquid, h_m is the latent heat of vaporization, a is a function of temperature, enthalpy of vaporization, and pressure of the vapor and liquid regions,[35] and the pressure variation within the liquid region is assumed to be negligible. The equation predicts a higher evaporation rate at regions of higher T_{lv} or smaller thickness δ, similar to that observed from the MD simulations at the base of the bubble.

In summary, we have developed and validated a novel surface-heating algorithm for water in molecular dynamics simulations. The algorithm is used to heat water droplets at different platinum surface temperatures. The estimated contact angles of the droplets are found to be in good agreement with theory and experiments. The transient evaporation behavior of the droplet is studied and shown to conform to the Kelvin−Clapeyron equation. The algorithm also captures the proper heat diffusion within water based on a comparison with the analytical solution

DOI: 10.1021/acs.jpclett.5b01627
J. Phys. Chem. Lett. 2015, 6, 3765−3769

of the one-dimensional heat equation. Furthermore, the algorithm is computationally efficient and easy to implement. It can be extended to other surfaces and can also be used to simulate differential thermal regions on the same surface without much complexity. The algorithm provides the capability to simulate various phenomena, such as nanoscale evaporation, Leidenfrost effect, and so forth, that involve the evaporation (or condensation) of water droplets and thin films.

■ ASSOCIATED CONTENT

Supporting Information

The Supporting Information is available free of charge on the ACS Publications website at DOI: 10.1021/acs.jpclett.5b01627.

Zhu Philpott (ZP) potential, validation of the surface heating algorithm with a one-dimensional heat equation, and pseudo code of the algorithm are discussed in detail (PDF)

■ AUTHOR INFORMATION

Corresponding Author

*E-mail: scmaroo@syr.edu.

Funding

This material is based upon work supported by the National Science Foundation under Grant No. 1454450.

Notes

The authors declare no competing financial interest.

■ REFERENCES

(1) Berendsen, H. J.; Postma, J. P. M.; Van Gunsteren, W. F.; DiNola, A.; Haak, J. Molecular Dynamics with Coupling to an External Bath. *J. Chem. Phys.* **1984**, *81*, 3684−3690.

(2) Nosé, S. A Unified Formulation of the Constant Temperature Molecular Dynamics Methods. *J. Chem. Phys.* **1984**, *81*, 511−519.

(3) Liem, S. Y.; Brown, D.; Clarke, J. H. Investigation of the Homogeneous-Shear Nonequilibrium-Molecular-Dynamics Method. *Phys. Rev. A: At., Mol., Opt. Phys.* **1992**, *45*, 3706.

(4) Van Der Spoel, D.; Van Maaren, P. J. The Origin of Layer Structure Artifacts in Simulations of Liquid Water. *J. Chem. Theory Comput.* **2006**, *2*, 1−11.

(5) Abraham, F. F. The Interfacial Density Profile of a Lennard-Jones Fluid in Contact with a (100) Lennard-Jones Wall and its Relationship to Idealized Fluid/Wall Systems: A Monte Carlo Simulation. *J. Chem. Phys.* **1978**, *68*, 3713−3716.

(6) Bernardi, S.; Todd, B.; Searles, D. J. Thermostating Highly Confined Fluids. *J. Chem. Phys.* **2010**, *132*, 244706.

(7) Yi, P.; Poulikakos, D.; Walther, J.; Yadigaroglu, G. Molecular Dynamics Simulation of Vaporization of an Ultra-Thin Liquid Argon Layer on a Surface. *Int. J. Heat Mass Transfer* **2002**, *45*, 2087−2100.

(8) Maroo, S. C.; Chung, J. Molecular Dynamic Simulation of Platinum Heater and Associated Nano-Scale Liquid Argon Film Evaporation and Colloidal Adsorption Characteristics. *J. Colloid Interface Sci.* **2008**, *328*, 134−146.

(9) Shi, B.; Dhir, V. K. Molecular Dynamics Simulation of the Contact Angle of Liquids on Solid Surfaces. *J. Chem. Phys.* **2009**, *130*, 034705.

(10) De Luca, S.; Todd, B.; Hansen, J.; Daivis, P. J. A New and Effective Method for Thermostatting Confined Fluids. *J. Chem. Phys.* **2014**, *140*, 054502.

(11) Hu, H.; Sun, Y. Effect of Nanopatterns on Kapitza Resistance at a Water-Gold Interface During Boiling: A Molecular Dynamics Study. *J. Appl. Phys.* **2012**, *112*, 053508.

(12) Mao, Y.; Zhang, Y. Molecular Dynamics Simulation on Rapid Boiling of Water on a Hot Copper Plate. *Appl. Therm. Eng.* **2014**, *62*, 607−612.

(13) Wang, S.; Tu, Y.; Wan, R.; Fang, H. Evaporation of Tiny Water Aggregation on Solid Surfaces with Different Wetting Properties. *J. Phys. Chem. B* **2012**, *116*, 13863−13867.

(14) Qiu, B.; Bao, H.; Zhang, G.; Wu, Y.; Ruan, X. Molecular Dynamics Simulations of Lattice Thermal Conductivity and Spectral Phonon Mean Free Path of PbTe: Bulk and Nanostructures. *Comput. Mater. Sci.* **2012**, *53*, 278−285.

(15) Saha, S. K.; Shi, L. Molecular Dynamics Simulation of Thermal Transport at a Nanometer Scale Constriction in Silicon. *J. Appl. Phys.* **2007**, *101*, 074304.

(16) Berendsen, H.; Grigera, J.; Straatsma, T. The Missing Term in Effective Pair Potentials. *J. Phys. Chem.* **1987**, *91*, 6269−6271.

(17) Pronk, S.; Páll, S.; Schulz, R.; Larsson, P.; Bjelkmar, P.; Apostolov, R.; Shirts, M. R.; Smith, J. C.; Kasson, P. M.; Van Der Spoel, D. GROMACS 4.5: A High-Throughput and Highly Parallel Open Source Molecular Simulation Toolkit. *Bioinformatics* **2013**, *29*, 845.

(18) Andersen, H. C. RATTLE: A Velocity Version of the SHAKE Algorithm for Molecular Dynamics Calculations. *J. Comput. Phys.* **1983**, *52*, 24−34.

(19) Zhu, S. B.; Philpott, M. R. Interaction of Water with Metal Surfaces. *J. Chem. Phys.* **1994**, *100*, 6961−6968.

(20) Maroo, S. C.; Chung, J. A Novel Fluid−Wall Heat Transfer Model for Molecular Dynamics Simulations. *J. Nanopart. Res.* **2010**, *12*, 1913−1924.

(21) Raj, R.; Maroo, S. C.; Wang, E. N. Wettability of Graphene. *Nano Lett.* **2013**, *13*, 1509−1515.

(22) Taherian, F.; Marcon, V.; Van Der Vegt, N. F.; Leroy, F. d. r. What is the Contact Angle of Water on Graphene? *Langmuir* **2013**, *29*, 1457−1465.

(23) Sergi, D.; Scocchi, G.; Ortona, A. Molecular Dynamics Simulations of the Contact Angle between Water Droplets and Graphite Surfaces. *Fluid Phase Equilib.* **2012**, *332*, 173−177.

(24) Werder, T.; Walther, J. H.; Jaffe, R. L.; Halicioglu, T.; Noca, F.; Koumoutsakos, P. Molecular Dynamics Simulation of Contact Angles of Water Droplets in Carbon Nanotubes. *Nano Lett.* **2001**, *1*, 697−702.

(25) Werder, T.; Walther, J. H.; Jaffe, R.; Halicioglu, T.; Koumoutsakos, P. On the Water-Carbon Interaction for Use in Molecular Dynamics Simulations of Graphite and Carbon Nanotubes. *J. Phys. Chem. B* **2003**, *107*, 1345−1352.

(26) Hong, S. D.; Ha, M. Y.; Balachandar, S. Static and Dynamic Contact Angles of Water Droplet on a Solid Surface using Molecular Dynamics Simulation. *J. Colloid Interface Sci.* **2009**, *339*, 187−195.

(27) Grigera, J. R.; Kalko, S. G.; Fischbarg, J. Wall-Water Interface. A Molecular Dynamics Study. *Langmuir* **1996**, *12*, 154−158.

(28) Hirvi, J. T.; Pakkanen, T. A. Molecular Dynamics Simulations of Water Droplets on Polymer Surfaces. *J. Chem. Phys.* **2006**, *125*, 144712.

(29) Kimura, T.; Maruyama, S. Molecular Dynamics Simulation of Water Droplet in Contact with a Platinum Surface. *Heat Transfer* **2002**, *1*, 537−542.

(30) Y. D., S.; Maroo, S. C. A New Algorithm for Contact Angle Estimation in Molecular Dynamics Simulations. ASME InterPACK & ICNMM: San Francisco, 2015.

(31) Thomas, S. M.; Chan, Y. A Simple Approach for the Estimation of Circular Arc Center and its Radius. *Computer Vision, Graphics, and Image Processing* **1989**, *45*, 362−370.

(32) Young, T. An Essay on the Cohesion of Fluids. *Philo. Trans. of the Royal Society of London* **1805**, *95*, 65−87.

(33) Laplace, P. S. Traité de Mécanique Céleste. *de l'Imprimerie de Crapelet*, **1805**; Vol. *4*.

(34) Kandlikar, S. G.; Steinke, M. E.; Maruyama, S.; Kimura, T. In *Molecular Dynamics Simulation and Measurement of Contact Angle of Water Droplet on a Platinum Surface*, Proc. of 2001; ASME IMECE: New York, 2001; pp 343−348.

(35) DasGupta, S.; Kim, I.; Wayner, P. Use of the Kelvin-Clapeyron Equation to Model an Evaporating Curved Microfilm. *J. Heat Transfer* **1995**, *2*, 128.

DOI: 10.1021/acs.jpclett.5b01627
J. Phys. Chem. Lett. 2015, 6, 3765−3769